Supporting Information

1. DFT Phase Diagram Formalism

The formalism of Norskov, *et al.*[1] for reference states/voltages is adopted using the reaction:

$$Pt_{slab} + nH_2O \rightarrow PtO(\theta) + nH_2 = PtO(\theta) + 2nH^+ + 2ne^- \quad [1]$$

where n is the number of oxygens that are adsorbed to the Pt slab and fractional coverage, θ, is given by:

$$\theta = n/n_{Pt} \quad [2]$$

where n_{Pt} is the number of Pt surface atoms in the Pt slab used. The Pt(111) slabs used are 5 layers thick with the bottom 2 layers frozen to simulate bulk with each layer containing either a 3x3 or 4x4 supercell of Pt atoms. All slabs contain a minimum of 15Å vacuum space to limit surface-surface interactions. Monkhorst-Pack k-point meshes of 6x6x1, and 4x4x1are used for 3x3 and 4x4 cells, respectively, to hold k-point density roughly constant across cell sizes. Projector augmented wave (PAW) pseudopotentials[2,3] are used with generalized gradient approximation exchange correlation functionals as parameterized by Perdew, Burke, and Ernzerhof [4,5]. Calculations are done with spin polarization and a plane wave cut off of 400eV. A convergence criteria for the electronic self-consistent optimization of 10^{-4} eV/cell was used. For the convergence of the geometric loop, a value of 10^{-3} eV/cell was used. From these calculations, we determine reaction energies by:

$$\Delta E_{VASP} = \left(E_{PtO(\theta)} + nE_{H_2}\right) - \left(E_{Pt,slab} + nE_{H_2O}\right) \quad [3]$$

$E_{PtO(\theta)}$ is the total ground state energy of the phase with fractional surface coverage θ, E_{H_2} is the ground state energy of an isolated H_2 molecule, $E_{Pt,slab}$ is the ground state energy of the Pt slab with no oxygen, and E_{H_2O} is the ground state energy of an isolated H_2O molecule. ΔE_{VASP} is used to calculate the Gibbs free energy of reaction at a given voltage and pH:

$$\Delta G = \Delta E_{VASP} + \Delta ZPE - T\Delta S - 2ne^-V - 2k_BT\ln(10)pH \quad [4]$$
$$= \Delta E_{VASP} + n(0.05eV) - 2ne^-V - 2k_BT\ln(10)pH$$

Which gives the binding energy (BE) per oxygen:

$$BE = \frac{\Delta G}{n} \quad [5]$$

V represents the applied potential vs. SHE and e^- is electron charge. We assume a constant shift in zero-point energy (ΔZPE) and entropy per oxygen adsorption reaction of 0.05 eV at 300 K[1] and ignore interactions with the electrolyte/water interface due to the relatively small dipoles formed on the surface of all systems calculated, consistent with previously reported studies[1,6]. The formation energy (FE) is calculated from the binding energy per oxygen of Equation 5 and is used in calculating the Pt/O surface convex hull:

$$FE = BE(\theta) - (1-\theta)BE_{\theta=0} - \theta BE_{\theta=1} \quad [6]$$

The end member at zero coverage is extrapolated from low coverage cells ($1/9^{th}$ and $1/16^{th}$ monolayers (ML)) using a linear fit to 1/L (L=3 and 4 for $1/9^{th}$ and $1/16^{th}$ ML, respectively) and is used as the zero of the binding energy scale. The 1 ML end member is taken to be that of a Pt slab with oxygen occupying all of the free FCC hollow sites above the slab.

Surface free energy per Pt surface site is calculated using Equation 7:

$$\gamma(\theta,V) = \theta BE(\theta,V) \quad [7]$$

A key assumption of this formalism is that the 0K DFT data may be extrapolated to room temperature. This extrapolation is reliable if the surface entropy (configurational and vibrational) is negligibly small, which is a reasonable assumption. A discussion on vibrational contributions to MoS_2 nanoparticle surface energies can be found in Ref. 7.

Another key assumption is the lack of OH adsorption at lower coverages. The lack of OH may affect the stability of the low coverage phases up to ¼ ML[8]. However, higher coverage phases should not be affected. In addition, as pointed out in Ref. 8, implications from Ref. 9 suggest that the electric field acts to destabilize OH relative to O on the Pt surface. These findings suggest that the OH phases are thermodynamically unstable with respect to pure O phases in the presence of an electric field. However, issues of kinetics, anion and water interactions, and DFT accuracy may mean that OH adsorption does still occur under experimental conditions.

2. Oxygen-oxygen Interaction

A Temkin or Frumkin like adsorption isotherm with a linear relation between oxide destabilization energy and fractional oxide coverage has been assumed in literature (discussed below) to describe the leveling out of the current in the anodic portion of CV at higher voltages. Similarly, previous work by Conway[10], Alsabet[11], and Jerkiewicz[12] suggest that in order to follow the experimentally observed logarithmic growth behavior, a linear interaction term (such as that of the Temkin and Frumkin isotherms) is required. Alsabet et al. find that this logarithmic behavior is rigorously followed up to 1.0V. Here we demonstrate that our Density Functional Theory (DFT) energies are consistent with a linear interaction term and that the magnitude of the interaction predicted from DFT is consistent with that found in experiments.

Darling and Meyers[13] have an effective interaction energy of 30 kJ/mol. They have treated this as a kinetic term, however, and, if we bring their interaction term inside the thermodynamic portion of their Butler-Volmer equation (with symmetry coefficient of 0.5), we would have an effective interaction energy of 60 kJ/mol. Holby *et al.*[14] found a similar value of 50 kJ/mol. Heyd and Harrington[15] do not formulate their reaction rate directly from a free energy but, if we use their "b" term of 0.06 $cm^{-2}\mu C^{-1}$, assume a surface charge of 220 μC/ML (their value), a symmetry factor of ½ and standard temperature conditions, an effective interaction term of 65 kJ/mol is calculated.

In order to make contact between this interaction term and the onset voltages found using DFT, we apply the following formalism. We follow previous works [13,14,16] and write the zero temperature free energy of reaction as in Equation 8:

$$\Delta G(\theta,V) = \Delta G_0 + \omega\theta - ne^- V \qquad [8]$$

This equation includes an oxide and voltage independent term (ΔG_0), a term linearly related to fractional oxide coverage (ω) and a voltage term that accounts for the electrons produced in oxide formation. The term ω can be estimated from the change in stable phase voltages with oxide coverage. The slope calculated in Fig. SI1 gives how the stable phase voltage changes as fractional oxide coverage is changed ($\chi = dV/d\theta$). Since these phases are the equilibrium phases at the given applied voltages, at that voltage and fractional coverage the free energy of reaction is zero. Separating Equation 8 and differentiating, we write at term relating the slope, χ ,and the oxygen-oxygen interaction term, ω:

$$\chi = \frac{dV}{d\theta} = \frac{\omega}{ne^-}; \omega = \chi ne^- \qquad [9]$$

Using the stable phases and their onset voltages, we perform a linear fit of onset voltage vs. fractional oxygen coverage. Applying the χ value of 0.57 V/ML (Fig. SI1), we find an effective interaction term of 110 kJ/mol, significantly higher than the 50-65 kJ/mol fitted for the kinetic rate models[14,15,17]. However, as discussed in the main text, it is likely that kinetics of the buckled phases inhibit their growth to some degree on the time scales of CV experiments. Furthermore, in fitting interactions all of the models utilized, at least partially, CV data with upper turning potentials well below the predicted onset voltage of the 1 ML phase (and some below the ¾ ML phase as well). Consequently, the low coverage portion of Fig. SI1 likely best describes the behavior being captured in the single interaction energy kinetic models. If only the first two points are used (those below 1.0V, the logarithmic range reported by Alsabet et al.), we find a slope of 0.29 V/ML (see Fig. SI2) corresponding to a ω value of 55 kJ/mol, directly in line with the values used in previous models that are based on fitting to CV curves. In the future, more sophisticated thermo-kinetic models may utilize the observed shifts in oxygen interaction energy determined using DFT at different phases to produce a more accurate CV model.

Overall, our phase diagrams confirm the use of a Temkin/Frumkin like isotherm for the Pt(111)/O system up to 1 ML but suggests some variation at higher coverages. We find a quantitatively similar oxygen-oxygen interaction energy compared with previous oxide formation models using low coverage phases that do not include buckling or place exchange.

We next consider the origins of this effective interaction energy. Alsabet et al.[11] suggest that the dipole of a PtO molecule measured in vacuum confirms their use of dipole-dipole interaction to describe this oxygen-oxygen repulsion term. Our DFT studies suggest that oxygen on a Pt surface has a dipole of 0.171D, roughly an order of magnitude below what they state to be required for place exchange to occur (1.3D). Thus, we conclude that the dipole interaction on the surface is too weak to drive place exchange. We propose that the electrostatic repulsion of the charged oxygen is likely responsible for the interaction energy.

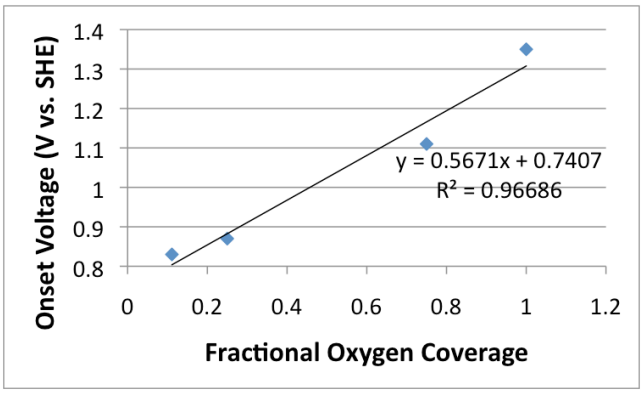

SI1. Onset voltage of stable phases vs. fractional oxygen coverage at pH=0 with linear fit.

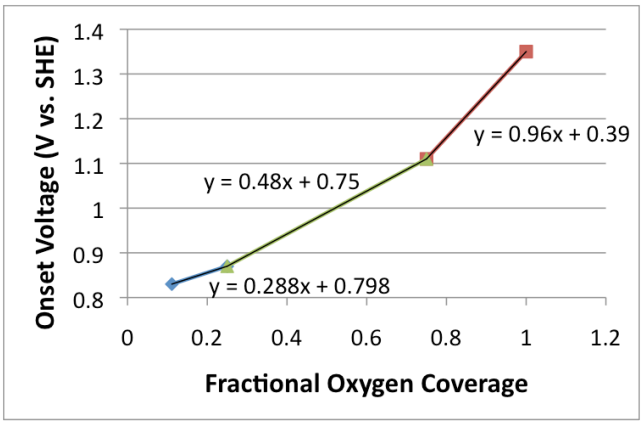

SI2. Same plot as Fig. SI1 but with each region fit independently to show variation in slope (0.29 V/ML, 0.48 V/ML, and 0.96 V/ML, corresponding to interaction values of 55 kJ/mol, 93 kJ/mol, and 185 kJ/mol).

3. VASP Energies

For ease of comparison, we give the calculated VASP energy values used in the making of Figure 1 below in Table SI1

Table SI1. VASP Enthalpies for phases plotted in Figure 1.

Surface FCC Hollow Site Occupation Phases

Name (coverage and cell size)	VASP Energy (eV)
1/16 - 4x4	-471.489
1/9 - 3x3	-267.803
2/9 2NN - 3x3	-273.698
1/4 slight buckle - 4x4	-489.459

1/4 - 4x4	-488.328
1/3 Clustered -3x3	-278.923
1/3 -3x3	-279.346
1/2 slight buckle - 4x4	-511.056
1/2 - 4x4	-510.487
2/3 -3x3	-294.142
3/4 - 4x4	-527.687
7/9 -3x3	-297.937
15/16 - 4x4	-538.875
1ML-4x4	-542.250

Buckled Phases (No Place Exchange)

Name (coverage and cell size)	VASP Energy (eV)
1/3 -3x3 Clustered	-278.923
1/2 - 4x4	-511.297
2/3 - 4x6 PtO2-like	-787.192
3/4 - 4x4 Hawkins	-533.386

Place Exchanged Phases

Name (coverage and cell size)	VASP Energy (eV)
1ML Hybrid 2 - 4x4	-553.435
1ML Hybrid 1 - 4x4	-551.565
1ML PtO2-like - 4x4	-549.712
Place Exchanged - 3x3	-305.423

4. Bader Charge Analysis

Through the use of Bader charge analysis, we identify an effective net charge associated with each atom. By considering the minimum of the electron density between two atoms, an effective volume (Bader volume) associated with each atom is generated. The electronic charge contained in such a volume is then attributed to the atom associated with that volume[18]. The density of states output is then analyzed using a code generated at the University of Texas-Austin[19-21]. The code devises Bader volumes and integrates the density of states to assign charged states to the atoms in the system. We find that in case of 3/4ML, the charge of buckled Pt is nearly identical with that of the PtO bulk phase. Going to the 1ML phase, however, the charge of the Pt is further increased for the Pt in the exchanged rows. This change is likely due to the presence of O below the surface, giving the top layer of Pt in the exchanged row a more PtO_2-like character.

Table SI2. Average change in atomic charge of atoms in the Pt bulk, PtO_2 bulk, 3/4ML phase of Hawkins *et al.,* and new hybrid 1ML phase from Bader charge analysis (change is relative to a reference case of 78 e^- for Pt (Pt atom) and 8 e^- for O (O atom)).

Atom - System	Avg. Change in Charge (e^-)	Deviation in Avg. Change in Charge (+/- e^-)
Pt -Pt Bulk	0.00	0.00
Pt - PtO	0.95	0.00
O - PtO	-0.95	0.00
Pt -α-PtO_2 bulk	1.62	0.00
O - α-PtO2 bulk	-0.81	0.00
Pt - β-PtO_2 bulk	1.70	0.00
O - β-PtO_2 bulk	-0.85	0.00
Pt - Hawkins 3/4 ML Buckled Row	0.95	0.00
O - Hawkins 3/4 ML Buckled Row	-0.71	0.01
Pt - Hybrid Exchanged Row	1.12	0.01
O - Hybrid Exchanged Row (top)	-0.62	0.02
O - Hybrid Exchanged Row (bottom)	-0.73	0.02
Pt - Hybrid Buckled Row	0.97	0.01
O - Hybrid Buckled Row	-0.73	0.01

SI REFERENCES

(1) Norskov, J. K.; Rossmeisl, J.; Logadottir, A.; Lindqvist, L.; Kitchin, J. R.; Bligaard, T.; Jonsson, H. *Journal of Physical Chemistry B* **2004**, *108*, 17886-17892.

(2) Kresse, G.; Joubert, D. *Physical Review B* **1999**, *59*, 1758-1775.

(3) Blochl, P. E. *Physical Review B* **1994**, *50*, 17953-17979.

(4) Perdew, J. P.; Burke, K.; Ernzerhof, M. *Physical Review Letters* **1996**, *77*, 3865-3868.

(5) Perdew, J. P.; Burke, K.; Ernzerhof, M. *Phys. Rev. Lett.* **1997**, *78*, 1396.

(6) Rossmeisl, J.; Norskov, J.; Taylor, C.; Janik, M.; Neurock, M. *Journal of Physical Chemistry B* **2006**, *110*, 218330-21839.

(7) Bollinger, M. V.; Jacobsen, K. W.; Norskov, J. *Physical Review B* **2003**, *67*.

(8) Hansen, H. A.; Rossmeisl, J.; Norskov, J. K. *Physical Chemistry Chemical Physics* **2008**, *10*, 3722-3730.

(9) Karlberg, G. S.; Rossmeisl, J.; Norskov, J. *Physical Chemistry Chemical Physics* **2007**, *9*, 5158-5161.

(10) Conway, B. E. *Progress in Surface Science* **1995**, *49*, 331-452.

(11) Alsabet, M.; Grden, M.; Jerkiewicz, G. *Journal of Electroanalytical Chemistry* **2006**, *589*, 120-127.

(12) Jerkiewicz, G.; Vatankhah, G.; Lessard, J.; Soriaga, M.; Park, Y. *Electrochimica Acta* **2004**, *49*, 1451-1459.

(13) Darling, R. M.; Meyers, J. P. *Journal of the Electrochemical Society* **2003**, *150*, A1523-A1527.

(14) Holby, E. F.; Sheng, W. C.; Shao-Horn, Y.; Morgan, D. *Energy & Environmental Science* **2009**, *2*, 865-871.

(15) Heyd, D. V.; Harrington, D. A. *Journal of Electroanalytical Chemistry* **1992**, *335*, 19.

(16) Holby, E. F.; Shao-Horn, Y.; Sheng, W.; Morgan, D. *ECS Transactions* **2009**, *25*, 583-592.

(17) Darling, R. M.; Meyers, J. P. *Journal of the Electrochemical Society* **2005**, *152*, A242-A247.

(18) Bader, R. F. W. *Atoms in Molecules*; Oxford University Press: Oxford, 1990.

(19) Tang, W.; Sanville, E.; Henkelman, G. *Journal of Physics: Condensed Matter* **2009**, *21*.

(20) Sanville, E.; Kenny, S. D.; Smith, R.; Henkelman, G. *Journal of Computational Chemistry* **2007**, *28*, 899-908.

(21) Henkelman, G.; Arnaldsson, A.; Jonsson, H. *Computational Materials Science* **2006**, *36*, 354-360.